JOURNAL OF GEOPHYSICAL RESEARCH, VOL. 104, NO. A9, PAGES 19,955–19,969, SEPTEMBER 1, 1999

Monitoring spatial and temporal variations in the dayside plasmasphere using geomagnetic field line resonances

F. W. Menk, [1,2,3] D. Orr, [4] M. A. Clilverd, [5] A. J. Smith, [5] C. L. Waters, [1,2]
D. K. Milling, [4] and B. J. Fraser [1,2]

Abstract. It is well known that the resonant frequency of geomagnetic field lines is determined by the magnetic field and plasma density. We used cross-phase and related methods to determine the field line resonance frequency across 2.4≤<L≤4.5 in the Northern Hemisphere at 78°-106° magnetic longitude and centered on L=2.8 in the Southern Hemisphere at 226° magnetic longitude, for several days in October and November 1990. The temporal and spatial variation in plasma mass density was thus determined and compared with VLF whistler measurements of electron densities at similar times and locations. The plasma mass loading was estimated and found to be low, corresponding to 5-10% He^+ on the days examined. The plasma mass density is described by a law of the form $(R/R_{eq})^{-p}$, where p is in the range 3-6 but shows considerable temporal variation, for example, in response to changes in magnetic activity. Other features that were observed include diurnal trends such as the sunrise enhancement in plasma density at low latitudes, latitude-dependent substorm refilling effects, shelves in the plasma density versus L profile, and a longitudinal asymmetry in plasma density. We can also monitor motion of the plasmapause across the station array. Properties of the resonance were examined, including the resonance size, Q, and damping. Finally, we note the appearance of fine structure in power spectra at these latitudes, suggesting that magnetospheric waveguide or cavity modes may be important in selecting wave frequencies.

1. Introduction

The purpose of this paper is to demonstrate the use of naturally occurring ULF oscillations of the geomagnetic field to monitor temporal and spatial variations in plasmaspheric density. This is possible because ULF energy within the magnetosphere can drive field line resonances (FLRs) at the local field line eigenfrequency [e.g., *Orr,* 1984], this frequency depending upon the plasma density in the region of space threaded by the field line. The oscillation frequency of the fundamental mode, ω_R, can be related to the plasma density ρ using the WKB time of flight approximation [*Obayashi and Jacobs,* 1958; *Warner and Orr,* 1979]:

$$\omega_R^{-1} \approx \frac{1}{\pi}\int \frac{ds}{v_A(s)} \qquad (1)$$

where $v_A(s) = B/(\mu_0\rho)^{1/2}$ is the Alfvén velocity along the resonant field line, μ_0 is the permeability of space, and B is the magnetic field strength. This approximation becomes unreliable when the oscillation wavelength is comparable to the scale size of the system, but it is convenient at high latitudes because distortions from a dipole magnetic field geometry can be readily incorporated.

[1] Department of Physics, University of Newcastle, Callaghan, New South Wales, Australia.
[2] Also at Cooperative Research Centre for Satellite Systems, Canberra, A. C. T., Australia.
[3] Also at Department of Physics, University of York, Heslington, England.
[4] Department of Physics, University of York, Heslington, England.
[5] British Antarctic Survey, Cambridge, England.

Paper number 1999JA900205.
0148-0227/99/1999JA900205$09.00

In an axisymmetric geometry populated by a uniform cold plasma, the magnetohydrodynamic wave which propagates parallel to the ambient magnetic field, called the shear Alfvén mode, corresponds to standing toroidal field line oscillations if the field line is terminated at each end by a reflecting boundary [*Tamao,* 1966; *Radoski,* 1972; *Orr,* 1984]. The oscillations are then described by

$$1 - k_z^2 v_A^2/\omega^2 = 0 \qquad (2)$$

where k_z is the parallel wave number.

The field line eigenfrequencies can be calculated using suitable plasma density and magnetic field models. One of the first to do this was *Obayashi* [1958], who considered three plasma density models of the form ρ = constant, $\rho = \rho_o R^{-6}$, and $\rho = \rho_s \exp(\alpha/R)$, where R is the geocentric distance and ρ_o, ρ_s, and α are parameters to be determined experimentally. *Cummings et al.* [1969] numerically calculated the toroidal mode eigenfrequencies of the first through sixth harmonics for a dipolar L=6.6 field line by representing the plasma density variation as R^{-p}, where p is a parameter in the range from 0 to 6 (the superscript p has been used here instead of the more familiar m to avoid confusion with azimuthal wave number). A two-component proton-electron plasma was assumed. Here-in-after we call p the mass density index. A value p=0 denotes constant plasma density with altitude, while p=6 indicates a constant Alfvén velocity profile. The modeling was extended by *Orr and Matthew* [1971], who computed eigenfrequencies over a range of latitudes. They used p=3 in the plasmasphere and p=4 in the plasma trough. Accurate analytic formulae for calculating the toroidal mode eigenfrequency were presented by *Taylor and Walker* [1984]. At low latitudes the plasma density model should include ionospheric mass loading [*Poulter et al.*, 1984a], and at high and low latitudes more realistic magnetic field models are necessary [*Singer et al.*, 1981; *Hattingh and Sutcliffe,* 1987].

Measurements of toroidal mode eigenfrequencies can be used to estimate magnetospheric plasma mass densities in the equatorial plane [e.g., *Troitskaya and Gul'yel'mi*, 1970; *Takahashi and McPherron*, 1982; *Takahashi and Anderson*, 1992]. However, it is not always easy to determine the resonant frequency at low latitudes, because the pulsation spectrum is dominated by the source mechanism [*Kurchashov et al.*, 1987]. One method for detecting a resonance is to identify the change in polarization occurring across the resonant field line. This was done by *Webb et al.* [1977] with an L=3.2-4.3 array of ground magnetometers. Resonant frequencies may be more conveniently determined using synchronous observations of pulsation power and phase between closely spaced ground magnetometers [*Baransky et al.*, 1985]. In this way, *Fedorov et al.* [1990] determined the equatorial plasma density profile over 3.0<L<4.5, with estimated uncertainties of order 10-40%.

At high latitudes, field line resonances can be detected by HF radars [*Walker et al.*, 1992], while plasma trough mass densities calculated from VHF radar observations have implied O^+ proportions in the range 30-70% [*Poulter et al.*, 1984b]. *Waters et al.* [1995] examined 10 weeks of data from the Canadian Auroral Network for the OPEN Program Unified Study (CANOPUS) magnetometer array with the cross-phase technique, and using the *Tsyganenko* [1987] field model, they were able to compare the observed temporal variation in resonant frequency with that expected for an R^{-4} density distribution in the plasma trough.

Additional information on the plasma distribution along a field line is available when harmonics of the FLRs are present [*Gul'yel'mi*, 1970; *Troitskaya and Gul'yel'mi*, 1970]. Thus *Takahashi and McPherron* [1982] were able to determine the temporal variation in ρ_{eq} (mass density in the equatorial plane) and the mass density index p by comparing the harmonic spacing at synchronous orbit with the toroidal mode eigenfrequency calculations of *Cummings et al.* [1969].

Lightning-generated VLF whistlers propagate along field-aligned paths and provide important information on magnetospheric electron density [e.g., *Carpenter and Smith*, 1964; *Park et al.*, 1978]. A related technique involves measuring the group delay and Doppler shift of ducted VLF whistler mode signals propagating along field lines between a suitable VLF transmitter and a conjugate receiver [*Thomson*, 1981; *Smith et al.*, 1987]. The transmission frequency restricts this technique to low latitudes (L<2.7), and because of absorption in the lower ionosphere, the signals are very difficult to detect in the daytime. Simultaneous measurement of more than one frequency at a receiver site allows accurate determination of the location of the flux tube footprint [*Clilverd et al.*, 1991]. Information on radial convective motion of flux tube plasma under the influence of transverse electric fields can be obtained from Doppler shift data [*Saxton and Smith*, 1989].

This paper presents observations of FLRs recorded at the foot of plasmaspheric field lines with two longitudinally separated arrays of ground magnetometers. Properties of the resonance, including the scale size, Q, and damping, and the appearance of fine spectral structure are discussed. Toroidal mode plasma density values are then calculated, and their diurnal, latitudinal, and longitudinal variation is examined for selected days. The mass density index p is determined from the observed harmonic spacing. The plasma mass densities are compared with electron densities found using natural VLF whistlers and the VLF group delay technique on selected days. *Webb et al.* [1977] had also compared ULF and VLF measurements of magnetospheric cold plasma and electron densities, for pulsation events recorded over 4 days. They found good agreement between the two methods but did not discuss mass loading or temporal or longitudinal trends, concluding that further ULF-VLF investigations were warranted. Accordingly, we demonstrate in this paper how ULF wave observations may be used to monitor the plasmaspheric density and its temporal and spatial variation. This is difficult to accomplish with spacecraft, whose rapid motion through these regions results in spectral broadening and phase shear [*Anderson et al.*, 1989]. The VLF whistler comparisons lend confidence to the ULF plasma density determinations and allow the plasma mass loading to be investigated.

2. Observations and Data Analysis

2.1. Magnetometer Stations and Measurement of Resonant Frequencies

Observations presented in this paper were obtained with the SAMNET (Sub-Auroral Magnetometer Network) array operated by the University of York, England, and two stations of the meridional low-latitude array operated by the University of Newcastle, Australia. The SAMNET digital fluxgate magnetometers sampled the geomagnetic H, D, and Z components every 5 s with a resolution of 0.25 nT; for further details, see the work of *Yeoman et al.* [1990] and the data available at http://samsun.york.ac.uk/samnet.html. Stations used for this study (YOR, GML, FAR, KVI, NUR, and OUL) are listed in Table 1. Corrected geomagnetic coordinates (CGM; available at http://nssdc.gsfc.nasa.gov/space/cgm/) are used throughout. At the first three stations, LT≈UT, and for the other three, LT≈UT+2. The Australian data were obtained with digital induction magnetometers featuring spectral correction over the 10-100 mHz range, sampled every 2 s with a resolution of order 0.1 nT; see the work of *Waters et al.* [1994] and the data available at http://plasma.newcastle.edu.au/spwg/. The stations used here (LAU and LEM) are also listed in Table 1; for these, LT≈UT+10. The remaining three stations in Table 1 are the VLF receiver sites discussed in section 2.4.

Techniques for determining field line eigenfrequencies were reviewed by *Menk et al.* [1994] and *Pilipenko and Fedorov* [1994]. We used the cross-phase method described by *Waters et al.* [1991] to produce whole-day spectra, which are well suited to examining temporal variations in the resonant frequency. The principles behind the cross-phase technique were first described by *Baransky et al.* [1989]. It is assumed that a resonance continuum exists throughout the magnetosphere. Over a suitably restricted section of the geomagnetic meridian, the properties of the resonance are determined by the spatial variation in amplitude and phase. The resultant phase difference between the H component at adjacent meridional magnetometer stations is evaluated, and the peak in the cross-phase spectrum then identifies the resonance approximately midway between the stations. The exact resonance location depends on how frequency varies with latitude. This method requires the magnetometers to exhibit identical amplitude, frequency, and phase response and precise timing.

The approximate midpoint L values for this study are given in the first two columns of Table 2, where it has been assumed that the resonant frequency varies linearly with L between adjacent stations. The YOR-GML and LAU-LEM pairs have the same midpoint L values, allowing comparison of FLR characteristics over 10 hours in local time. Cross-power information is used to provide threshold information when plotting cross-phase spectra.

The choice of station location for cross-phase measurements is a compromise between maintaining adequate signal coherence in the wave fields [*Waters et al.*, 1995] and resolving the peak in the cross-phase spectrum. This, in turn, depends on the rate at which the resonant frequency varies with latitude and on the damping

Table 1. Coordinates and L-Shell Values of Stations Used in This Study, Calculated Using the CGM at 100 km Altitude for Epoch 1990

		Geographic Coordinates, deg		Geomagnetic Coordinates, deg			
Station	Code	Latitude	Longitude	Latitude	Longitude	LT=UT+	L Shell
Launceston	LAU	-41.7	147.1	-53.0	225.6	9.81	2.80
Lemont	LEM	-42.3	147.5	-53.6	226.3	9.83	2.88
York	YOR	53.95	358.95	50.99	78.95	-0.07	2.56
Glenmore	GML	57.16	356.32	54.97	78.19	-0.25	3.08
Faroe Island	FAR	62.05	352.98	60.82	78.10	-0.47	4.27
Kvistaberg	KVI	59.50	17.63	56.04	96.39	1.18	3.25
Nurmijarvi	NUR	60.50	24.65	56.81	102.66	1.64	3.39
Oulu	OUL	65.10	25.85	61.54	105.91	1.72	4.47
Faraday		-65.3	295.7	-49.9	8.92	-4.29	2.44
Dunedin		-45.8	170.5	-53.1	255.3	11.37	2.81
Halley		-75.60	333.23	-61.46	28.57	-1.78	4.45

Faraday, Dunedin, and Halley are VLF receiver sites. CGM denotes corrected geomagnetic coordinates.

factor. Separations of the SAMNET stations (e.g., 5.9° for GML-FAR and 4.7° for NUR-OUL) are significantly larger than those in previous cross-phase studies [*Waters et al.*, 1991, 1995], raising the possibility of using these techniques with other existing magnetometer arrays. However, resonance signatures were not obtained on all days for the most widely spaced station pairs.

Cross-phase measurements are one of a suite of techniques for determining field line eigenfrequencies. *Baransky et al.* [1985] discussed methods which involve evaluating the ratio or the difference in the H component amplitude spectra between two nearby latitudinally separated stations, $H_P(f)/H_E(f)$ or $H_P(f)-H_E(f)$, respectively, where subscript P refers to the poleward station and E refers to the equatorward station of the pair. The FLR condition is then given by $H_P/H_E(f_R)=1$ and $H_P-H_E(f_R)=0$.

The resonant frequency at a particular station may also be determined from the ratio or difference in the H and D component powers or amplitude spectra [*Baransky et al.*, 1990; *Vellante et al.*, 1993]. This offers the advantage of not requiring accurate interstation phase or time information. It is assumed that resonance amplification results in a peak in the H component power spectrum relative to the D component. FLRs will thus be difficult to detect when the wave modes are coupled or the Q is low. *Green et al.* [1993] showed that resonant frequencies evaluated this way are not always the same as those found with the cross-phase or amplitude ratio methods.

Finally, *Waters et al.* [1995] pointed out that the coherence between the H components at closely spaced meridional stations, being estimated by smoothing the frequency domain, decreases near the resonant frequency, and this may help identify the resonant frequency. In this paper we have examined specific intervals using all of the above techniques in order to provide comparisons between them and to maximize the number of sample sites.

2.2. Intervals Examined

Magnetic pulsation data recorded over October 15 to November 5, 1990, were examined, being the period when the Australian stations were operating. The SAMNET array has operated continuously since 1989. Time series plots, filtered over the range 5-100 mHz, and whole-day dynamic power spectra were first examined for all days and stations. Eight of these days were then selected for detailed analysis. For this purpose, H component cross-spectral power and phase were computed using a Fast

Table 2. Resonance Properties on October 16, 1990

Code	Midpoint L Value	Resonant Frequency f_R, mHz (±0.5)	Phase Peak $\Delta\varphi$, deg	Resonance Width ε, * x10^2 km	Resonance Q *
LAU-LEM	2.8	15.4	20 ± 5	2.7 (2.1-3.7)	5.3 (3.9-6.8)
YOR-GML	2.8	14.9	92 ± 27	1.7 (1.1-2.6)	5.1 (3.4-8.0)
KVI-NUR	3.2	13.8	30 ± 10	1.6 (1.1-2.5)	6.4 (4.0-9.0)
GML-FAR	3.7	12.1	97 ± 37	2.1 (1.1-3.0)	6.3 (4.3-12)
NUR-OUL	3.9	10.7	110 ± 27	1.3 (0.8-1.9)	19 (13-32)

* Numbers in parentheses indicate 1 standard deviation.

Fourier transform (FFT) and a sliding time window either 21 min (SAMNET) or 17 min (LAU-LEM) long, stepping through the data with 3.75 and 4.00 min long increments, respectively, to construct whole-day dynamic spectra. The data were first detrended and weighted by multiplying the power by f^n, where n is in the range 1.0-2.0. To facilitate FLR detection, the cross-phase peak may be enhanced by raising it by some convenient power in a process analogous to that described by *Olson and Samson* [1980] for Stokes vector-based detectors. The FLR frequency was measured each hour at each station pair where the characteristic cross-phase signature was apparent and consistent with the cross-power spectra.

A number of factors influenced the choice of stations and days for detailed analysis. The ground stations spanned the range $2.5<L<4.5$. At these latitudes, mass loading due to ionospheric O^+ should have little influence on the integrated plasma density [*Poulter et al.*, 1988], stations are equatorward of the plasmapause under average quiet conditions, and a dipole field can be assumed. The plasmapause location was estimated following *Orr and Webb* [1975]. The days selected had consistent, moderate to low K_p over that and the previous day and exhibited FLRs with reasonable power at LAU-LEM and YOR-GML. These days are October 16, 17, and 18 and November 1, 2, 3, and 4, 1990.

2.3. Calculation of Equatorial Mass Densities

Two methods were used to calculate equatorial mass densities from the measured field line eigenfrequencies. The equation for the toroidal mode eigenfrequency described by *Orr and Matthew* [1971] was used for model distributions of the form $(R/R_{eq})^{-2}$, $(R/R_{eq})^{-3}$ and $(R/R_{eq})^{-4}$, where R is the geocentric distance along the field line [e.g., *Walker and Russell*, 1995, Figure 6.1] and R_{eq} is the distance to the equatorial crossing point of the field line. The choice of value for the mass density index has been discussed by many authors, including *Carpenter and Smith* [1964], *Gul'yel'mi* [1966], and *Singer et al.* [1981]. The calculation was performed for each hour and station or station pair at which FLRs were observed on one representative day, October 16, 1990. For comparison, mass densities were then recalculated with the $(R/R_{eq})^{-3}$ analytical formula described by *Taylor and Walker* [1984] and *Walker et al.* [1992]. This yielded essentially identical results to the previous $(R/R_{eq})^{-3}$ estimates and was then used to calculate plasma mass densities for each hour of data from each station or station pair for all the other days. The uncertainty in the calculated mass densities depends mainly on the resolution in measuring the resonant frequency and is of order 10-15%. We have ignored uncertainties due to the plasma density and magnetic field models; these are discussed in section 5.2. The Earth's dipole moment was taken as $M_E=7.84\times10^{15}$ T m^3.

2.4. VLF Measurements of Plasmaspheric Electron Density

Equatorial electron densities, N_{eq}, were obtained using the ducted VLF experiment described by *Thomson* [1981], *Smith et al.* [1987], and *Clilverd et al.* [1991]. The measured VLF group delays, t_g, are approximately proportional to $\sqrt{N_{eq}}$. Electron densities were calculated using a diffusive equilibrium model with height-dependent temperature profiles along the field lines [*Mahajan and Brace*, 1969]. Thus no short-term ionospheric variations are considered. This is reasonable for the latitudes of interest as most of the VLF group delay arises from the equatorial region. In turn this means the technique is relatively insensitive to the choice of low-altitude model.

Duct locations were determined for two longitude sectors. VLF Doppler receivers at Faraday, Antarctica (see Table 1), received ducted whistler mode signals from two U.S. Navy transmitters (NAA, 24.0 kHz, at Cutler, Maine; and NSS, 21.4 kHz., at Annapolis, Maryland). The receivers were described by *Thomson* [1981] and are able to separate the whistler mode signals from the stronger subionospheric signal, providing measurements of the group delays and Doppler shifts of the whistler mode component [*Saxton and Smith*, 1989]. Similar receivers at Dunedin, New Zealand, detected signals from NLK (24.8 kHz, at Seattle, Washington) and NPM (23.4 kHz, at Hawaii). The Faraday receivers monitor the region 4-5 hours west of SAMNET, and the Dunedin receivers monitor the LAU-LEM longitude sector. Ducts for VLF propagation are formed by field-aligned density enhancements which are of order 10% above ambient [*Smith and Angerami*, 1968; *Angerami*, 1970]. The physics of duct formation was discussed in detail by *Cole* [1971] and *Walker* [1978].

Electron densities were also estimated for L shells beyond L=2.7 using natural VLF whistlers recorded at Halley Station (Table 1) and scaled using the technique of *Ho and Bernard* [1973]. These authors also discussed the errors in evaluating N_{eq} with whistler measurements, which are of order 5%. An extensive VLF whistler study of electron density in the plasmasphere was presented by *Park et al.* [1978].

The relationship between the observed plasma mass densities and short-term variations in ionospheric electron density was examined using hourly f_oF2 values from Hobart (geographic 32.92° S, 147.32° E; L=2.9) and Juliusruh/Rugen (geographic 54.60° N, 13.40° E; L=2.7). These data were obtained from World Data Centre C1 for Solar-Terrestrial Physics.

3. Case Studies

3.1. Properties of the Resonance

To illustrate the use of cross phase for monitoring FLRs, two representative intervals occurring on October 16, 1990, are considered. The first interval is 1130-1200 UT, when K_p=2-, and the second is 0810-0840 UT, when K_p=3+. We anticipate that the plasmapause moved poleward between these times, probably near or past L=4.5. Magnetic pulsation activity during both intervals is typical of that on all days studied.

An overview of activity on this day is given in Figure 1, where whole-day cross-phase spectra are presented for LAU-LEM, YOR-GML and GML-FAR. The fundamental and second-harmonic FLR signatures are visible at LAU-LEM in the form of broad horizontal bands around 16 and 40 mHz after about 1600 and 1900 UT, respectively (actually the next morning in local time). These bands denote cross phase between LAU and LEM of ~15°-20°. The fundamental FLR is also seen ~16 mHz from 0000 to 0500 UT. At YOR-GML the fundamental FLR signature is present in the form of patches ~14 mHz from 0800 to 1800 UT and at GML-FAR ~10 mHz between 0600 and 1600 UT. The narrow bands varying between 20 and 28 mHz at YOR-GML and at ~36 mHz at GML-FAR are instrumental artifacts. The cross-phase scale for LAU-LEM is different than that for the other pairs because the closer station spacing results in a smaller cross-phase peak at resonance. For the more widely spaced stations the lower coherence results in noisier cross-phase spectra. The phase resolution of the plots shown in Figure 1 is considerably poorer than that for the actual color versions used in the data analysis. The two selected intervals are indicated by triangles.

Detrended H component time series for the 1130-1200 UT interval are presented in Figure 2a. Latitude-dependent pulsations are superimposed upon larger oscillations at the SAMNET stations, although signals at YOR are dominated by the instrumental noise. For this reason it is difficult to identify the resonant

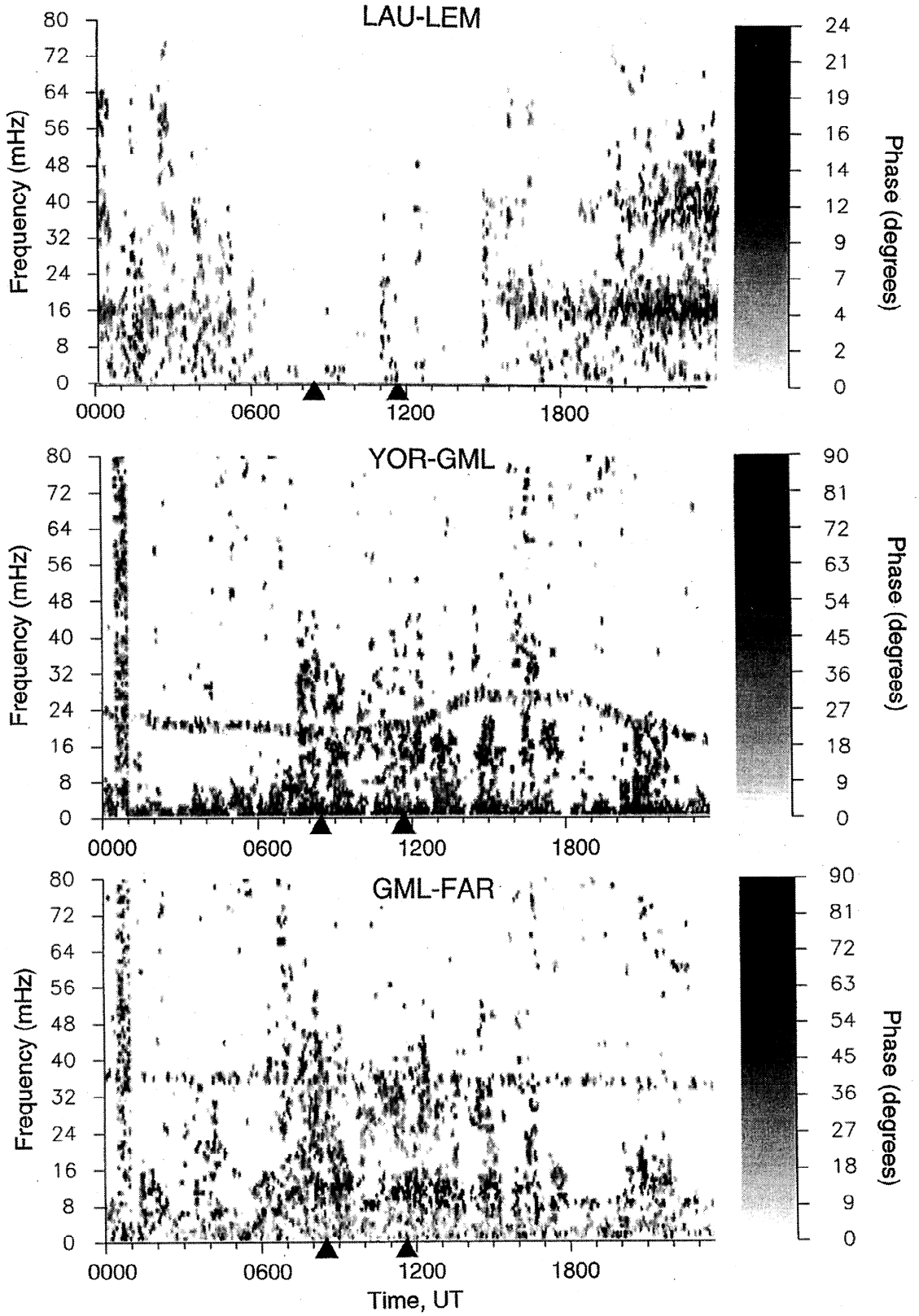

Figure 1. Whole-day dynamic cross-phase spectra for October 16, 1990, from LAU-LEM, YOR-GML, and GML-FAR.

frequency there using techniques such as complex demodulation [*Beamish et al.,* 1979]. LAU is in the pre-midnight sector, characterized by irregular long-period waveforms. The plot for LEM is very similar to that for LAU and therefore not shown. The corresponding normalized power spectra are presented in Figure 2b. A peak at 8-9 mHz occurs across the SAMNET array, with further peaks around 11 mHz (KVI and NUR) and 14-16 mHz (GML, KVI, NUR, FAR, and OUL). The large peak ~20 mHz at YOR is the artifact. LAU shows noise-like activity.

Interstation power and phase information for this interval is presented for representative station pairs in Figure 2c. For each station pair, the top plot shows the normalized amplitude-time

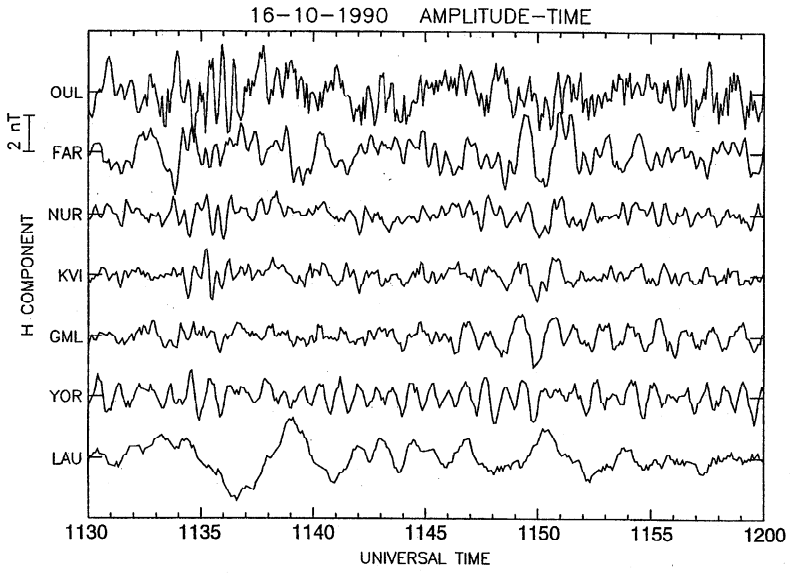

Figure 2a. Stacked time series for 1130-1200 UT, October 16, 1990. The *H* component is shown, band-pass-filtered over 5-50 mHz. Latitude increases from bottom to top.

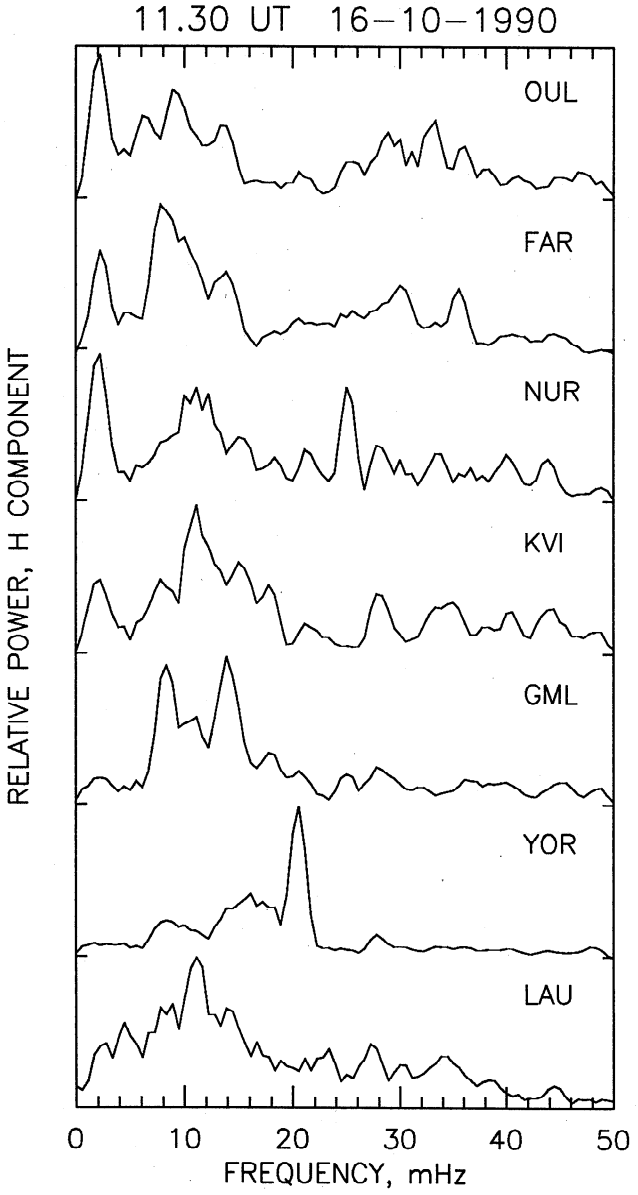

series for both stations. The next plot shows the cross power (solid curve) and coherence (dotted curve) between these series; the plot below that, shows the power difference (solid curve) and power ratio (dotted curve) spectra; and the bottom plot shows the cross-phase spectrum. The time series were high-pass-filtered at 5 mHz, and the spectra were weighted by $f^{1.0}$. In each case the resonance has been identified as described in section 2.1 and is labeled by an arrow. Frequency resolution is ±0.5 mHz. In general, where the coherence is low (<0.5), large irregular fluctuations may occur in the cross-phase, power difference, and power ratio spectra, and the data are considered unreliable. With the scaling used, the power difference and ratio traces often lie on top of each other.

Static spectra such as these are only a "snapshot" approximation to the actual spectrum. This is because of the variability in pulsation signals on timescales comparable to the FFT length, probably related to their wave packet nature, which tends to be averaged out in the whole-day spectra [*Verõ et al.*, 1998]. Resonant frequencies were therefore evaluated by joint comparison of static spectra such as those shown in Figure 2c and of dynamic spectra such as those illustrated in Figure 1.

Several interesting features are evident in Figure 2c. The resonance signature is clear in each case. For YOR-GML this is seen ~16 mHz, despite the very large noise band around 20 mHz. The ability to resolve FLRs whose power is small compared to nearby signals is one of the advantages of the cross-phase technique. No resonance signature can be identified for this interval for LAU-LEM (not shown). For GML-FAR the resonance is ~13 mHz. Note also the closely spaced peaks near this frequency in the cross-power spectrum. This is a fairly common feature, discussed further in section 5.1. The magnitude of the cross-phase peak for KVI-NUR is less than that for the other station pairs because of their small meridional separation (~90 km). The cross phase may also be affected by any azimuthal wave propagation effects between KVI and NUR, whose east-west separation is ~400 km. This may be assessed by inspecting the *D* component cross-phase spectrum, not shown here, which indicates an azimuthal wave number $m \approx 5$ (eastward propagation) at the resonant frequency.

Figure 2b. Normalized power spectra for the same time and stations as those in Figure 2a.

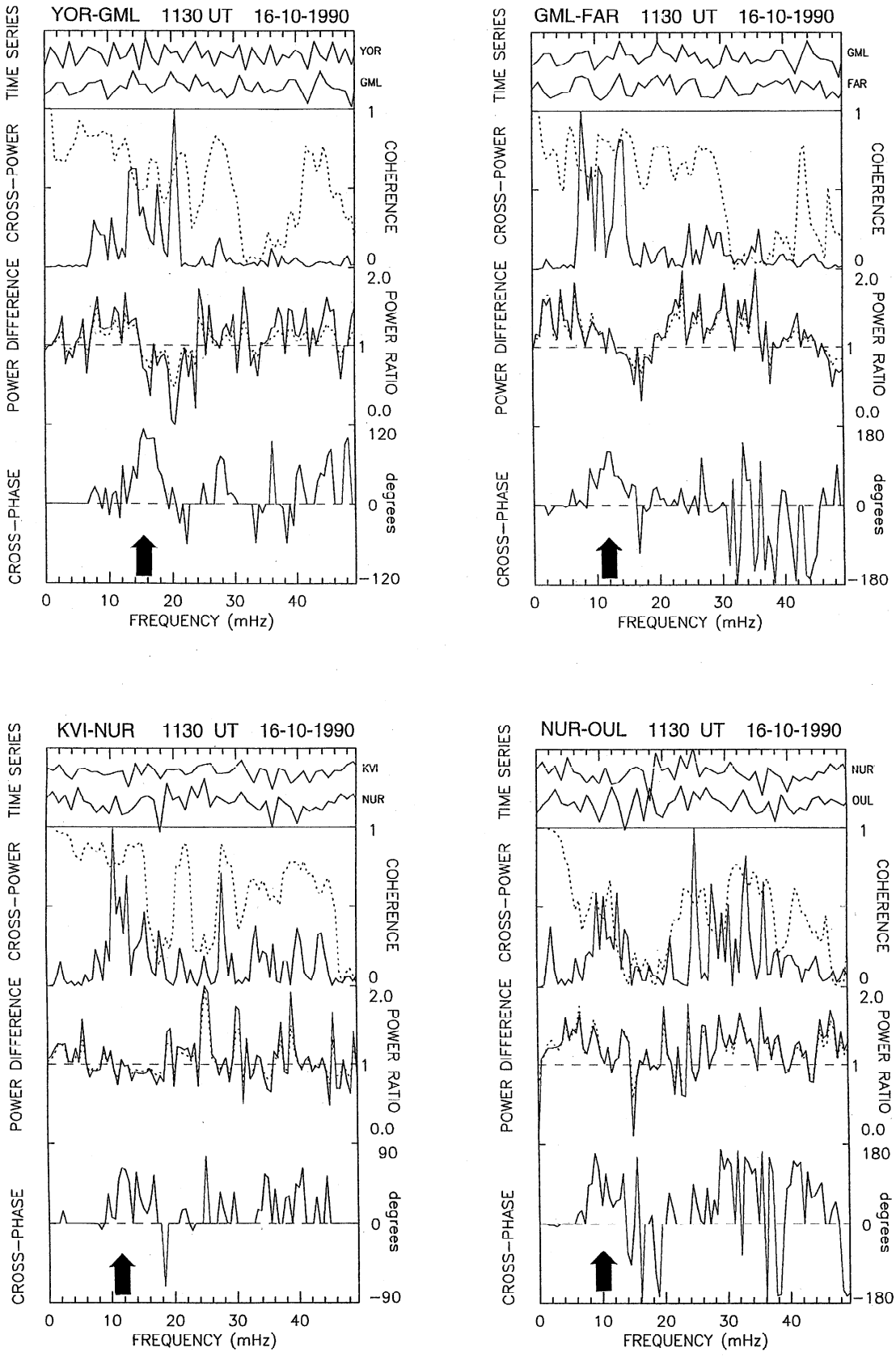

Figure 2c. Amplitude and phase information between station pairs for the interval 5-50 mHz. See text for details.

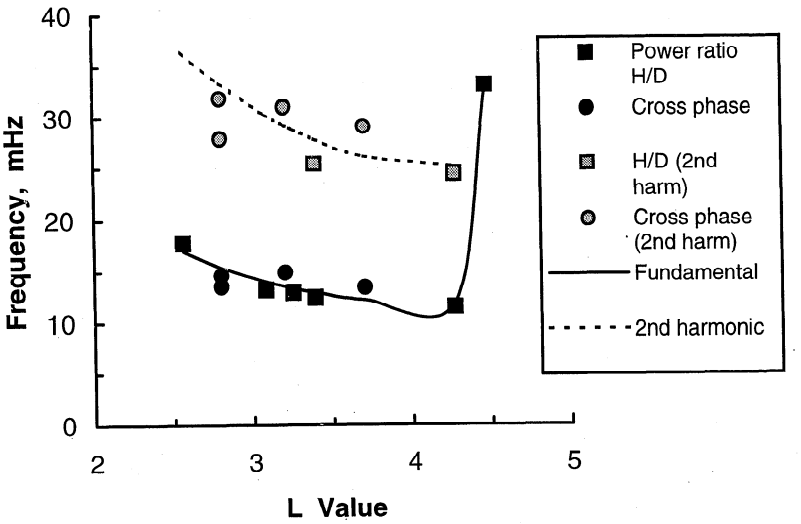

Figure 3. Variation in resonant frequency with latitude for a typical interval (0810-0840 UT, October 16, 1990), determined using cross phase and *H/D* ratio.

The final plot is for the NUR-OUL station pair. Although the coherence is low at higher frequencies, a resonance signature is present near 10 mHz. The whole-day dynamic power spectrum for OUL (not given) shows intervals of intense Pc3 pulsation activity, centered on 33 mHz, between 0730 and 1230 UT. This is consistent with previous observations at the plasmapause [*Orr and Matthew*, 1971]. The observations suggest that the plasmapause is near but most likely just poleward of OUL (L=4.47) during the 1130 UT interval.

Further insight on these aspects can be gained by examining the 0810-0840 UT interval in a similar manner. For brevity the plots are not presented here, but they show resonance signatures at all station pairs (including LAU-LEM) except NUR-OUL. This suggests a distortion of the eigenfrequency-latitude profile between NUR (L=3.39) and OUL (L=4.47), indicative of the presence of the plasmapause. The observations therefore suggest that the plasmapause moved poleward past L=4.5 between ~ 0840 and 1130 UT.

The power ratio, frequency gradient, and peak cross-phase value for each station pair may be used to estimate parameters of the resonance [*Green et al.*, 1993; *Menk et al.*, 1994; *Pilipenko and Fedorov*, 1994; *Waters et al.*, 1994]. Accordingly, Table 2 lists the resonant frequency f_R, peak cross-phase value at resonance, $\Delta\varphi$, characteristic half width, ε, and resonance Q, averaged over several intervals on October 16. Numbers in parentheses indicate 1 standard deviation. These results are discussed further in section 5.1.

The variation in resonant frequency with latitude for the 0810-0840 UT interval is illustrated in Figure 3. Fundamental and second-harmonic frequencies were determined using cross-phase and power difference information and the *H/D* spectral ratio. These techniques give similar (but not necessarily identical) results, although it is considerably easier to monitor temporal variations using cross-phase spectra. The solid and dashed curves represent best fits to the observations. In agreement with the cross-phase observations, the *H/D* results suggest that the plasmapause was located between L=4.3 and L=4.5 during this interval.

3.2. Plasma Mass Density Comparisons

The plasma mass densities derived from the fitted resonant frequency curves in Figure 3 are plotted in Figure 4 using solid, dashed, and dotted curves. The open circles are comparison

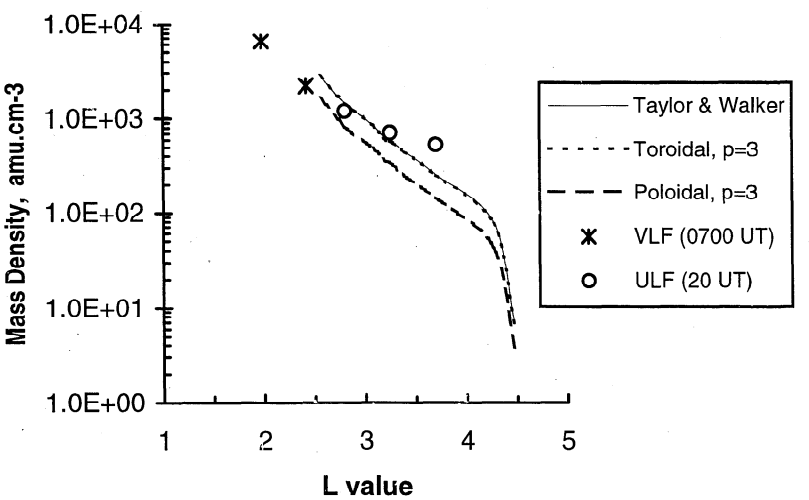

Figure 4. Equatorial plasma mass densities obtained using magnetometer power and cross-phase data and three models, for the interval shown in Figure 3. Electron densities from ducted VLF observations are represented by stars; circles denote densities based on ULF pulsation values at 2000 UT.

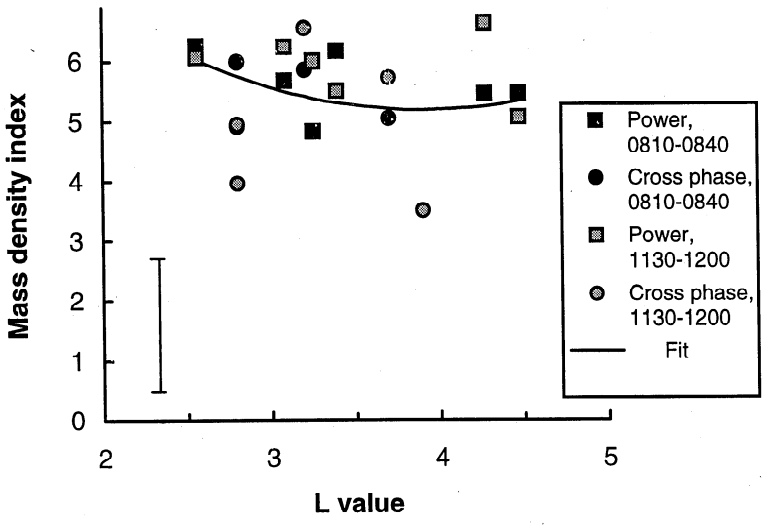

Figure 5. Latitudinal variation in mass density index p for the interval shown in Figure 3. The symbols are the same as those used in Figure 3.

observations discussed in section 4.3. Three models have been used in these calculations, the *Taylor and Walker* [1984] model with an R^{-3} profile and the *Orr and Matthew* [1971] toroidal and poloidal models also both with an R^{-3} profile. In reality, wave modes are coupled, so the actual densities should fall somewhere between the toroidal and poloidal mode calculations. Comparison with other plasma density power laws (R^{-4}, etc.) using the Orr and Matthew models shows that differences at any point are not significantly greater than the uncertainty. Henceforth all mass densities have been calculated using the Taylor and Walker R^{-3} model.

Two sets of VLF electron density measurements are available at 0700 UT, represented in Figure 4 by the stars. The first is for an L=2.42 duct near 298.2° geographic longitude (i.e., ~0253 LT) with N_{eq}= 2200 cm^{-3}, and the second is an L=1.98 duct near 309.3° geographic longitude (~0337 LT) with N_{eq}=6500 cm^{-3}. These values agree well with equatorial electron densities determined in a statistical survey by *Park et al.* [1978]. There is also reasonable agreement with the mass densities obtained from the FLR measurements, although the VLF values are from ducts 3-5 hours west of SAMNET. Comparison of these values allows the plasma mass loading to be estimated. This is discussed in section 5.3. The plasmapause is indicated by the sudden decrease in mass density at L>4. A more closely spaced station array would allow the precise position, shape, and temporal behavior of the plasmapause to be monitored.

The mass density index p was determined for both selected intervals using the *Cummings et al.* [1969] computations and the ratio of the fundamental and second-harmonic frequencies. The results are shown in Figure 5, where the solid curve represents the best fit averaged over both intervals and the symbols have the same meaning as those in Figure 3. The same procedure can be conducted using the ratio of the third and first harmonics. Figure 5 shows that for the times considered the mass density index is in the range 5-6 and may exhibit a slight variation with radial distance inside the plasmasphere. In turn this means that the FLR-derived densities represented in Figure 4 should be reduced by 10-20%.

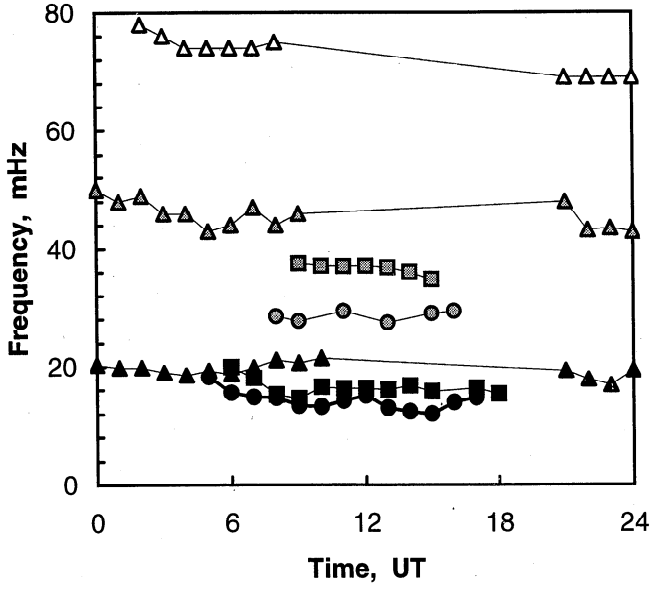

Figure 6. Variation in field line resonance frequency with time and latitude for October 22, 1990. Symbols represent the following station pairs: circles, GML-FAR (L=3.7); squares, YOR-GML (L=2.8); triangles, LAU-LEM (L=2.8).

4. Spatial and Temporal Variation in Plasma Density

4.1. Spatial and Temporal Variation in Resonant Frequency

Resonant frequencies were measured over 8 days as described in section 2.1 and plotted against time for all stations and pairs. For brevity only the plot for October 22, 1990, is presented here, in Figure 6. In each case, frequencies were determined using cross-phase spectra and *H/D* power ratios, for the fundamental mode (solid symbols) and higher harmonics (shaded and open symbols). The spectral resolution results in an error of order 5-6%, less than the width of the symbols, for each measurement. The highest K_p occurred on October 16 ($\sum K_p$=19); the average K_p over the 8 days examined was 2.2, and the lowest estimated plasmapause latitude was L=3.6, equatorward of FAR and OUL (during 0000-0300 UT, October 16, and 0000-0600 UT, November 1).

A number of trends were apparent in the whole-day plots, as follows: (1) Resonant frequencies at L=2.8 were sometimes very

similar or even identical across nearly 10 hours in local time (i.e., between LAU-LEM and YOR-GML), except near sunrise in either hemisphere. (2) However, on some days there were systematic differences between the LAU-LEM and YOR-GML (L=2.8) resonant frequencies (e.g., October 22, Figure 6) or in the frequency of a higher harmonic. (3) A pronounced decrease in resonant frequency following sunrise on some days indicates the effects of flux tube refilling from the ionosphere associated with O^+ production [*Poulter et al.*, 1988; *Waters et al.*, 1994]. This was observed for both the LAU-LEM and YOR-GML pairs, but the effect was larger in the Southern Hemisphere. (4) The variation in resonant frequency with latitude generally followed that shown in Figure 3, except that the L=3.7 (GML-FAR) resonance frequency was particularly low on November 4, the lowest K_p day, and the resonant frequencies at all stations tracked changes in K_p.

4.2. Longitudinal and Temporal Variation in Plasma Mass Density

For each station on each day the measured resonant frequency was used to calculate the effective equatorial plasma mass density. Electron densities were obtained from VLF observations of ducts at similar L values and times. Again, only the plot for October 22 is shown, in Figure 7. Both longitudinal or interhemispheric and temporal effects are apparent in Figure 7. Considering first longitudinal or interhemispheric effects, daytime densities for YOR-GML (357° geographic longitude) were up to 2.5 times higher than those for LAU-LEM (147° longitude, e.g., as seen in Figure 7 for October 22). To investigate this further, the ratio in plasma mass density between different longitudes in the Northern and Southern Hemispheres, $\rho_{N/S}$, was compared with the corresponding ratio in F region critical frequency, $f_oF2_{N/S}$, measured at nearby observatories, for three local times. The ratios were averaged over the 4 days on which this enhancement was observed, and the results are listed in Table 3. Errors denote 1 standard deviation. In each case the Northern Hemisphere f_oF2 value is higher than that for the Southern Hemisphere at the same local time, but the mass density ratios are larger. However, on another 4 days (October 16 and 17, and November 3 and 4) the $\rho_{N/S}$ values were very similar to the $f_oF2_{N/S}$ values for the same stations and times. The f_oF2 ratios were the same on both sets of days. The second set of observations suggests that while electron densities are slightly higher in the Northern Hemisphere, these are associated with a correspondingly higher plasma mass density. The mass density relates to the equatorial plane, and it is not clear whether its enhancement is connected with the higher ionospheric production rate in the Northern Hemisphere or a longitudinal effect. However, the first set of observations (those in Table 3) shows that on other days the mass densities were even further enhanced, and this must be due to additional factors. This points to a longitudinal effect and is discussed further in section 5.3.

Table 3. Ratio of Plasma Mass Density and f_oF2 at Northern and Southern Hemisphere Sites Separated by 10 Hours in Local Time, Averaged Over October 18 and 22 and November 1 and 2, 1990

Interhemispheric Ratio	0700 LT	1200 LT	1600 LT
$\rho_{N/S}$	1.6 ± 0.2	1.9 ± 0.4	1.8 ± 0.3
$f_oF2_{N/S}$	1.1 ± 0.2	1.4 ± 0.1	1.3 ± 0.1

Errors denote 1 standard deviation.

Considering temporal effects, our principal observations are summarized as follows:

1. Small magnetic storms occurred on October 15 and 31 (maximum K_p=5- in each case) and refilling was indicated by systematically increasing mass densities for one or more days afterward. The rate of increase was greater and occurred for a longer time at higher latitudes. This is illustrated for November 1-4 ($\sum K_p$=17.0, 18.0, 13.0, and 5.0) in Figure 8.
2. On days when there was little variation in K_p the mass density exhibited diurnal variations similar to the predictions of *Poulter et al.* [1988]. These results are discussed further in section 5.4.

4.3. Comparison Between ULF and VLF Measurements

It is instructive to compare VLF electron density measurements with the ULF FLR-derived mass density estimates. Two days are considered, the first being October 22, illustrated in Figure 7. The daytime L=2.8 FLR mass densities on this day were ~1.4×10^3 amu cm^{-3} at 357° longitude and ~0.83×10^2 amu cm^{-3} at 147° longitude. Ducted VLF measurements were available for four times between

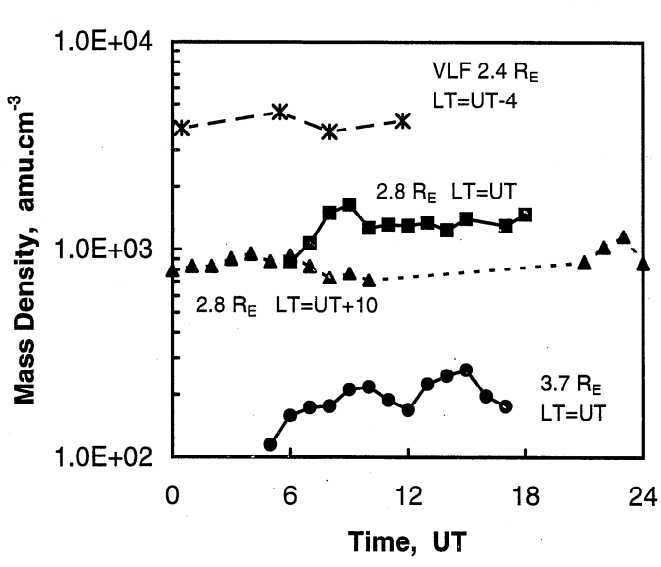

Figure 7. Variation in equatorial plasma mass density with time and latitude for October 22, 1990. The symbols are the same as those used in Figure 6.

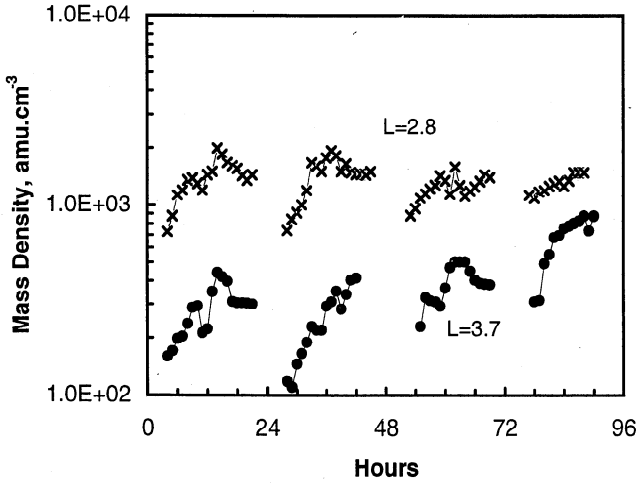

Figure 8. Plasma mass density at 2.8 and 3.7 R_E, 357-064° longitude, November 1-4, 1990. Time axis shows hours since 0000 UT on November 1.

0029 and 1144 UT, at an L=2.3-2.4 duct footprint near 292° longitude. When extrapolated to L=2.8 using an appropriate power law, these indicate that electron density decreased from 2.2 to 1.8×10^3 electrons cm^{-3} between 2048 and 0347 LT and then increased to ~2.1×10^3 cm^{-3} by 0736 LT. These results are consistent with diurnal duct depletion and filling. The VLF electron densities are higher than the ULF plasma mass densities for this day; this is discussed in section 5.3.

The second day considered here is October 16. Natural VLF whistlers were recorded at Halley Bay at 2005 UT (1821 LT) arriving from five different ducts. The resultant estimated electron densities ranged from 1.5×10^3 cm^{-3} at L=2.73 to 0.94×10^3 cm^{-3} at L=3.0. These values lie on top of the R^{-3} toroidal mode plots shown in Figure 4 for earlier on the same day. The corresponding ULF-derived mass densities for the same time are represented in Figure 4 by open circles. While the plasma density at 2000 UT exhibits a more gradual decrease with increasing latitude than it does at 0800 UT, there is good agreement between the VLF- and ULF-derived densities in both cases. These results are also discussed further in section 5.3.

5. Discussion

5.1. Structure of the Resonance

Here we discuss the appearance of resonance structure in cross-phase spectra. Relevant factors include the station separation, the variation in frequency and phase with latitude, the width and Q of the resonance, and the damping factor γ. The magnitude of the cross-phase peak at resonance depends on the station separation and the frequency gradient with geomagnetic latitude, $\partial f_R/\partial\Phi$. For large station separations the cross-phase peak flattens out, leading to uncertainty in evaluating the resonant frequency. The damping factor affects the rate at which cross phase varies with latitude near the resonance and the height of the maxima and minima in the power subtraction spectrum.

The cross-phase technique assumes that a continuum of FLRs is present throughout the plasmasphere, and it may be argued that this is unrealistic. In fact, the variation in phase with latitude associated with the resonance of a single field line [*Hughes and Southwood*, 1976] also produces a cross-phase peak for two closely spaced stations straddling the resonant field line. However, this does not explain why we see resonance signatures simultaneously across an array of stations. Spacecraft observations of the variation in toroidal mode frequency with radial distance suggest that a continuum of resonances is present throughout the magnetosphere at least at some times [e.g., *Takahashi and McPherron,* 1982; *Engebretson et al.,* 1986; *Takahashi and Anderson,* 1992]. Furthermore, resonance structure is apparent in ground cross-phase spectra even when there is little power at those frequencies [*Waters et al.,* 1991], demonstrating that field line eigenoscillations can be excited by low-level ULF power in the magnetosphere.

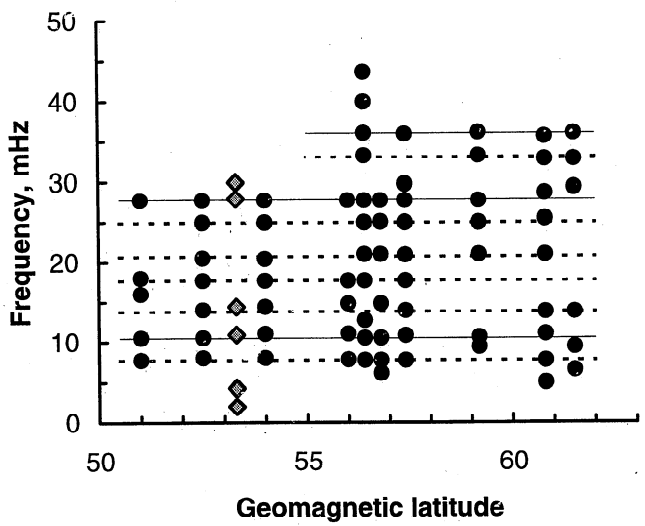

Figure 9. Frequency and latitude of significant peaks in the power spectra, 1130-1200 UT, October 16, 1990. See text for details.

Spacecraft motion limits the spatial resolution of low-altitude in situ studies. Detailed examination of power and cross-power spectra (e.g., Figure 2) reveals that closely spaced multiple peaks are often present. A clearer picture of this frequency structuring is provided by Figure 9, where the frequency of each main peak in the power spectra during the 1130-1200 UT October 16 interval is plotted against latitude. Dashed and solid curves indicate frequencies which were common across the array in the H and D components, respectively. Diamonds denote spectral peaks at LAU in the opposite hemisphere. The average frequency spacing is 3.2 ± 0.6 mHz (1 standard deviation), similar to that reported at lower latitudes [*Samson et al.,* 1995; *Verõ et al.,* 1998; *Menk et al.,* 1999]. Many instances of this spectral fine structuring have been observed. Because of the different sampling rates, different spectral parameters (FFT length, etc.) were used for the SAMNET and Australian stations, so it is unlikely that the fine structuring is a spectral artifact. This suggests the existence of quantized frequencies over the range $2.8 \leq L \leq 4.5$, in agreement with observations at L<2.0 [*Samson et al.,* 1995; *Verõ et al.,* 1998; *Menk et al.*, 1999]. These have been interpreted as evidence of discrete resonances driven by magnetospheric waveguide or cavity modes [*Samson et al.,* 1995; *Waters et al.,* 1999]. The discrete resonance spectrum would be superimposed upon the continuum spectrum which is probed using the cross-phase technique.

The resonance widths shown in Table 2 are of order 0.2-0.3 L, in agreement with previous results [*Green et al.,* 1993; *Menk et al.,*1994]. *Waters et al.* [1994] also demonstrated that the damping coefficient and hence Q depend on the relationship between the driving frequency and the resonant frequency. With the exception of NUR-OUL the Q values obtained here are of order 5-6, and the corresponding damping coefficients $\gamma/\omega_R \sim 0.1$. These agree with previous estimates [*Waters et al.,* 1994]. The anomalous values for NUR-OUL suggest that the observations may have been affected by some lateral geological inhomogeneity near OUL, although we have no other evidence of this. *Green et al.* [1993] suggested that such a geoelectric effect results in a dc bias in the amplitude subtraction and ratio spectra, as seen in Figure 2. However, modeling by *Waters et al.*, [1999] has shown that similar offsets can arise simply as a consequence of the mixing together of nearby discrete resonant frequencies.

The cross-phase method assumes that the resonant frequency varies homogeneously with latitude between adjacent stations. This will be invalid if structures such as the plasmapause are present between the stations of interest. The observations presented in section 3.1 show that movement of the plasmapause can be monitored in this way. It would be interesting to use a more closely spaced station array than the 1990 SAMNET configuration to monitor the location, shape, extent, and motion of the plasmapause. This is now under way and will be reported in a future paper.

The opposite problem arises with KVI-NUR, where the azimuthal variation in phase may be contributing to the cross-phase measurement. The D component cross-phase spectrum sometimes contains features not present in the H component cross-phase spectrum but which may be seen in the H component power

spectrum. This indicates the presence of nonresonance features. In fact, for longitudinally separated stations the whole-day cross-phase spectra can be relabeled in terms of wave number m to provide a convenient means of monitoring variations in azimuthal phase.

5.2. Plasma Density Modeling

The calculation of equatorial plasma mass density using observed resonant frequencies makes several assumptions: (1) that adjacent field lines are decoupled, (2) that the extreme cases of purely toroidal or poloidal mode oscillations are thus realistic, (3) that the plasma is collisionless, (4) that number density follows a simple law of the form $\rho=\rho_{eq}(R/R_{eq})^{-p}$, (5) that the magnetic field along the field line is accurately represented, and (6) that the density calculations relate to the equatorial plane. For these reasons such calculations are normally regarded as approximate. *Singer et al.* [1981] discussed many of these issues and derived a single exact linear wave equation for transverse (toroidal and poloidal modes) oscillations, which was solved in a realistic magnetospheric field geometry. Their comparisons with dipole model calculations showed that the latter are acceptable inside L~6. However, *Hattingh and Sutcliffe* [1987] considered that a more realistic magnetic field model, such as International Geomagnetic Reference Field (IGRF), is necessary at low latitudes. *Waters et al.* [1994] found that this provided a 10% difference compared to the dipole model at L=1.8. Figure 11 of *Poulter et al.* [1988] shows that around 30° latitude a guided wave spends most of its travel time in the O^+-dominated low-altitude regions, while at the higher latitudes considered in this paper the travel time, and hence resonant frequency, is determined by the Alfvén speed in the equatorial plane.

The agreement between the ULF mass densities and the VLF electron densities, shown in sections 3.2 and 4.2, demonstrates that none of the assumptions about the representation of the oscillation mode or the field model have had a significant effect. In particular, Figure 4 shows that the toroidal mode approximation is a reasonable one. The results also indicate that for the intervals examined the plasma is well approximated by a pure proton and electron regime, in agreement with the modeling of *Poulter et al.* [1988].

The mass density index p has been evaluated for all the stations and days examined and exhibits considerable variation. It was hoped to observe systematic temporal or spatial variations which may be connected with plasma redistribution processes, but usually there is large scatter in the observations. Results for one representative day, November 2, are shown in Figure 10. Note the size of the error bar. For LAU-LEM (triangles) the second and third harmonics ("2f" and "3f") were available on this day and produced good agreement. The mass density index is initially constant, p~5, and then decreases sharply to p~2, increasing again in the local morning of the next day at LAU-LEM. The similarity of the mass density indices, and hence harmonic ratios, at L=3.7 (GML-FAR, circles) and L=2.8 (YOR-GML, squares) agrees with Figure 10 of *Poulter et al.* [1988], where the harmonic ratio was modeled as a function of latitude.

The agreement in Figure 10 between the LAU-LEM and YOR-GML results around 0600-0800 UT indicates that the same power law was appropriate over 10 hours in local time. For a constant second- harmonic frequency and varying fundamental frequency, a variation in p from 3 to 6 or from 1 to 3 at L=2.8 requires a change in plasma mass density of only ±2%. It is therefore not surprising that the mass density index is a highly variable parameter, and the actual value chosen in model calculations probably is not critical. On the day shown, K_p decreased from 4- to 2- between 0300-0600 and 0600-0900 UT and increased again from 1+ to 2 between 1200-1500 and 1500-1800 UT. The observed variation in p thus may be associated with minor variations in plasmaspheric dimensions and the consequent redistribution of ionization.

Of course, plasma density models of the form $\rho=\rho_{eq}(R/R_{eq})^{-p}$ ignore the ionosphere and are inappropriate at low latitudes. *Waters et al.* [1994] discussed the use of the diffusive equilibrium, international reference ionosphere (IRI), and the *Bailey* [1983] models in this regard. A detailed comparison of these and other models and their validity has been presented by *Price et al.* [1999]. In general, the effect of H^+ in the equatorial plane dominates ionospheric O^+ at latitudes >40° [*Poulter et al.*, 1988], so we may regard our results as being reasonable.

5.3. Comparison of Mass Densities and Electron Densities and Longitudinal Effects

Comparing the ULF mass densities with the VLF electron densities allows an estimate of the mass loading. Using the results presented in Figure 7 for October 22, ~0730 LT, at L=2.8, the ratio of the mass density to the electron density is ~0.6. This is unreasonable unless (1) the plasma and/or electron density models are incorrect or (2) there is a longitudinal variation in plasma density. In fact, *Clilverd et al.* [1991] showed that a longitudinal effect is likely to be present in equatorial electron densities. This is a consequence of the annual variation in f_0F2, which is greatest around 300° longitude and arises from the combined effect of thermospheric winds and photoionization during summer in the Southern Hemisphere where the magnetic latitude is low but the geographic latitude is high. For an L=2.5 field line the annual variation in N_{eq} is ~3:1 at 300° geographic longitude, ~2:1 at 180° longitude, and negligible at 50° longitude. The October values are a significant fraction of these extremes. Accordingly, we may expect to find higher plasma densities for YOR-GML (~357° longitude) than for LAU-LEM (~147° longitude) in our results. This is seen in Figure 7 and was also found on other days. The VLF electron density data shown in Figure 7 are from 292° longitude, where we expect maximum enhancement owing to the longitudinally dependent annual variation. This may account for the electron densities being higher than the plasma densities.

Looking at data for October 16, the ducted VLF results for L=2.0 (309° longitude) and L=2.4 (298° longitude) at 0700 UT

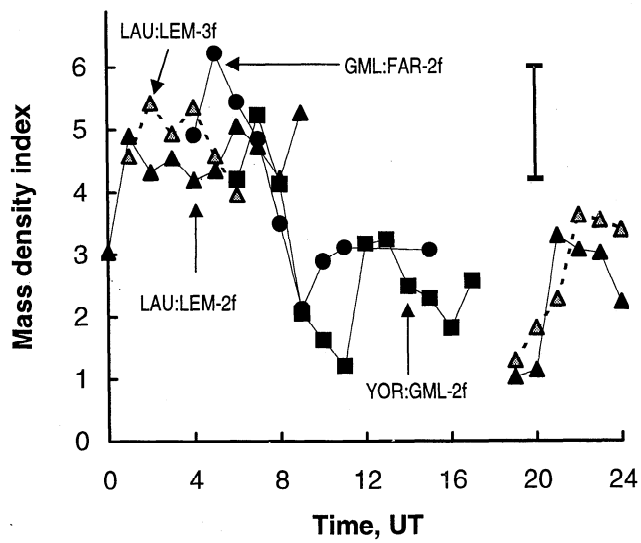

Figure 10. Variation in plasma density power law index with time and latitude on November 2, 1990. Symbols are the same as those for Figure 6.

(~0300 LT) relate to electron densities of 1.0-1.3 x 10^3 cm^{-3} at L=2.8. Similarly, the natural VLF observations at 2000 UT (~1800 LT; 333° longitude) also correspond to electron densities of 1.3 x 10^3 cm^{-3} at L=2.8. Comparing with the L=2.8 ULF plasma densities for 357° longitude averaged over this day gives a mass loading of order 1.1-1.2. This could be accounted for by a plasma comprising 95% H^+ and 5% He^+. There are a number of sources of uncertainty in this estimate. First, the longitudinal variation in electron density means that at the ULF flux tube the corresponding electron density is probably somewhat lower than it is at the VLF duct longitude. Second, we ignored the fact that an electron whistler duct is formed by a field-aligned electron density enhancement believed to be of order 10% (section 2.4). Third, in comparing the ULF- and VLF-derived densities we are actually comparing results from two different plasma density models, in this case of the form R^{-3} and $R^{-3.9}$, respectively. The first two effects mean that the inferred mass loading is probably an underestimate, while the third introduces only a small error.

5.4. Temporal Variations in Plasma Density

A qualitative description of plasmaspheric processes was presented by *Park et al.* [1978]. Briefly, thermal plasma is provided from the ionosphere, mainly in the form of H^+ (O^+ ions are too heavy to reach high altitudes and yield H^+ ions through a charge exchange reaction). Plasmaspheric filling commences at sunrise and occurs throughout local daytime, although cross-L drift can also provide a significant contribution [*Poulter et al.,* 1988]. Plasma may be lost through downward flow at night or during magnetic storms and through large-scale convection electric fields which sweep flux tubes into open field regions. During magnetic disturbances the size and density of the plasmasphere decrease, and plasma is most likely removed to the outer magnetosphere [*Smith and Clilverd,* 1991]. Refilling from the ionosphere is accomplished within ~ 1-2 days at L=2.5 [*Smith and Clilverd,* 1991] but takes ~8 days at L=4 [*Park,* 1974]. This is long enough that the outer plasmasphere rarely, if ever, reaches saturation level and is in a continual state of refilling after the previous disturbance.

Park et al. [1978] also presented an extensive statistical survey of electron density in the plasmasphere. The main results that concern us here are as follows:

1. Electron density-latitude profiles often show a ledge or some other change around L=3.5-4 associated with the transition from the saturated inner plasmasphere to the more dynamic recovering outer plasmasphere.

2. Under quiet conditions the equatorial electron density exhibits a diurnal variation of ~2 at L=2.5 and ~1.5 at L=3.0 [see also *Smith and Clilverd,* 1991]. Beyond L=3 diurnal effects are obscured by storm and substorm-associated effects.

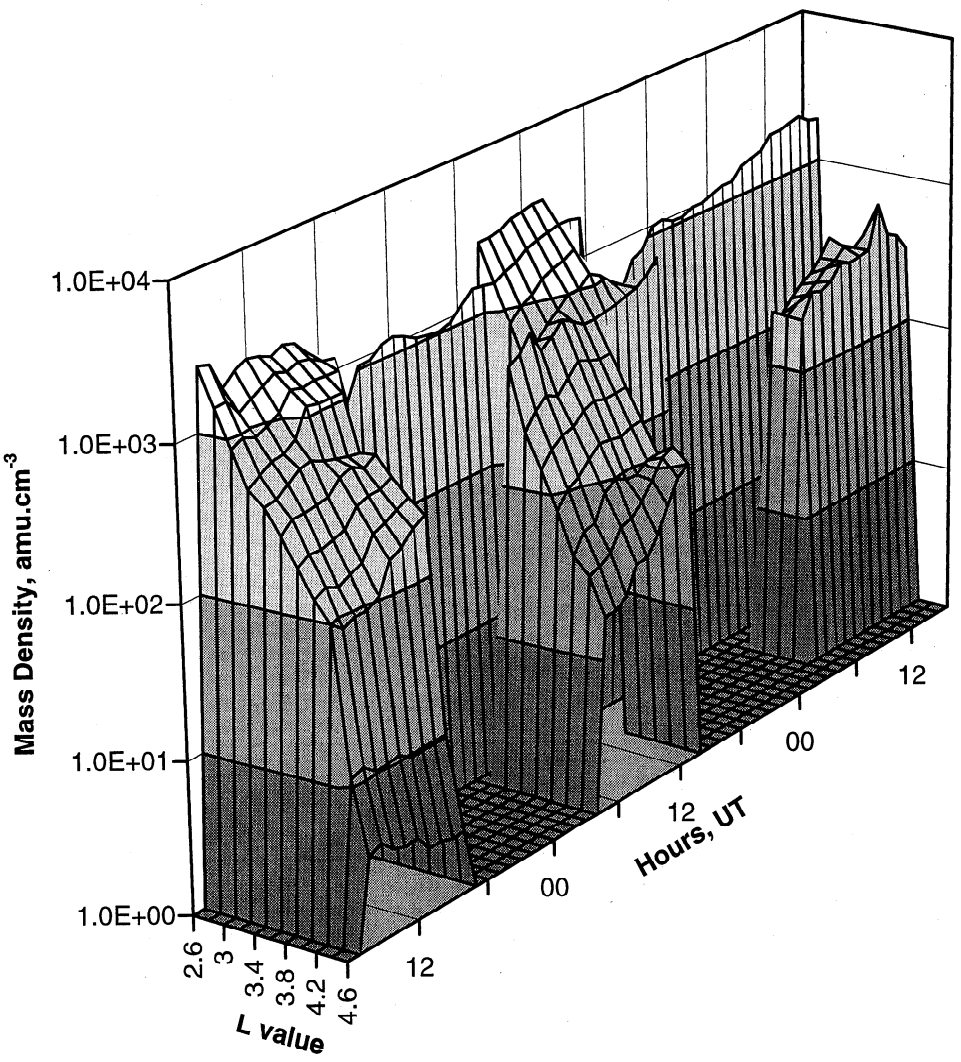

Figure 11. Plasma mass density map for October 16-18, 1990, from L=2.6 to L=4.6.

3. Plasmaspheric electron densities at L~2.5 are ~ 1.5 times higher at solar maximum compared to solar minimum, but no corresponding effect is seen beyond L~3. A solar cycle trend was previously reported for low-latitude ULF pulsation eigenfrequencies by *Vellante et al.* [1996].

Comparing the ULF-derived plasma mass density at stations with the same latitude but different local time (YOR-GML versus LAU-LEM) highlights diurnal variations, especially near dawn. *Poulter et al.* [1988] showed that at >40° latitude, E x B drift processes dominate chemical processes in the diurnal variation of pulsation eigenperiods. The azimuthal electric field convects flux tubes to different latitudes, and the resultant change in flux tube volume alters the plasma pressure and density. The modeled toroidal mode eigenfrequency thus decreases at sunrise, and for higher latitudes (L≥4) it increases again near noon (this increase is not seen at lower latitudes). This model describes the diurnal variation in FLR frequency and mass density observed on quiet days reasonably well (e.g., Figure 8). The latitude-dependent nature of the refilling process is also prominent in Figure 8.

Many of the plasmaspheric features described above are apparent in the ULF density data. These are illustrated in Figure 11, which shows a plasma density map for October 16-18, 1990, based on the FLR measurements discussed in section 4.2. Data from YOR-GML and LAU-LEM have been used to provide continuous coverage at L=2.8. Features which are apparent in this plot include (1) the sunrise increase in density at low latitudes, (2) the diurnal variation in density at low and higher latitudes, (3) plasmaspheric refilling occurring at a rate which depends on latitude, (4) a shelf in plasma density around L=4 on October 17, and (5) the longitudinal effect indicated by the discontinuities between the YOR-GML and LAU-LEM (L=2.8) values.

6. Conclusions

We have demonstrated the measurement of field line eigenfrequencies in the plasmasphere using ground magnetometer arrays and various techniques which exploit the variation in power and phase with latitude. The effective width, Q, and damping factor of the resonance have been evaluated over the range L=2.8-3.9 and are of order 0.2-0.3 L, 5-6, and γ/ω_R~0.1, respectively. These results complement and extend previous measurements. A more extensive magnetometer array would allow a picture of FLR properties across the entire magnetosphere to be constructed. For instance, it would be of particular interest to study the plasmapause region in this way. We have also found evidence of spectral fine structuring over L=2.8-4.5, which is similar to that observed at lower latitudes and which suggests that magnetospheric waveguide or cavity modes may be important in selecting wave frequencies.

Using the observed ULF eigenfrequencies, we have calculated the effective equatorial plasma mass densities with a simple R^{-3} model. Features which are present in the data include diurnal trends such as the sunrise enhancement in plasma density at low latitudes, latitude-dependent substorm refilling effects, shelves in the plasma density versus L profile, and interhemispheric and longitudinal differences in plasma density. The latter effect is also present in VLF electron density data. We have demonstrated how the mass density index can be monitored as a function of L and time and responds to changes in magnetic activity. Finally, we have shown how comparison of the ULF plasma density and VLF electron density results allows the mass loading to be determined. This was found to be low on the days examined, suggesting an He^+ proportion in the range 5-10%.

ULF pulsation data are available from many magnetometer arrays worldwide. This paper has demonstrated how such data sets may be used to monitor the dayside plasmasphere, although clearly this can also be extended to plasmapause and plasma trough latitudes. With both meridional and azimuthal magnetometer arrays (or groups of arrays), opportunities exist to examine both radial and local time variations in mass density. In principle, such measurements could be conducted in near real time.

Acknowledgments. SAMNET is operated by the University of York and supported by the U.K. Particle Physics and Astronomy Research Council (PPARC). Stations in Tasmania were operated by the University of Newcastle under programs supported by the Australian Research Council and the University of Newcastle. The VLF data were recorded under a program supported in part by the National Environment Research Council (U.K.). We thank N.R. Thomson for operating the VLF receivers in Otago. FWM received support from a PPARC Visiting Fellowship during this study.

Janet G. Luhmann thanks A.D.M. Walker and William Allan for their assistance in evaluating this paper.

References

Anderson, B. J., M. J. Engebretson, and L. J. Zanetti, Distortion effects in spacecraft observations of MHD toroidal standing waves: Theory and observations, *J. Geophys. Res., 94,* 13425, 1989.

Angerami, J. J., Whistler duct properties deduced from VLF observations made with OGO 3 satellite near the magnetic equator, *J. Geophys. Res., 75,* 6115, 1970.

Bailey, G. J., The effect of a meridional **E** x **B** drift on the thermal plasma at L=1.4, *Planet. Space Sci., 31,* 389, 1983.

Baransky, L. N., Y. E. Borovkov, M. B. Gokhberg, S. M. Krylov, and V. A. Troitskaya, High resolution method of direct measurement of the magnetic field lines' eigen frequencies, *Planet. Space Sci., 33,* 1369, 1985.

Baransky, L. N., S. P. Belokris, Y. E. Borovkov, M. B. Gokhberg, E. N. Fedorov, and C. A. Green, Restoration of the meridional structure of geomagnetic pulsation fields from gradient measurements, *Planet. Space Sci., 37,* 859, 1989.

Baransky, L. N., S. P. Belokris, Y. E. Borovkov, and C. A. Green, Two simple methods for the determination of the resonance frequencies of magnetic field lines, *Planet. Space Sci., 38,* 1573, 1990.

Beamish, D., H. W. Hanson, and D. C. Webb, Complex demodulation applied to Pi2 geomagnetic pulsations, *Geophys. J. R. Astron. Soc., 58,* 471, 1979.

Carpenter, D. L., and R. L. Smith, Whistler measurements of electron density in the magnetosphere, *Rev. Geophys., 2,* 915, 1964.

Clilverd, M. A., A. J. Smith, and N. R. Thomson, The annual variation in quiet time plasmaspheric electron density, determined from whistler mode group delays, *Planet. Space Sci., 39,* 1059, 1991.

Cole, K. D., Formation of field-aligned irregularities in the magnetosphere, *J. Atmos. Terr. Phys., 33,* 741, 1971.

Cummings, W. D., R. J. O'Sullivan, and P. J. Coleman Jr., Standing Alfven waves in the magnetosphere, *J. Geophys. Res., 74,* 778, 1969.

Engebretson, M. J., L. J. Zanetti, T. A. Potemra, and M. H. Acuna, Harmonically structured ULF pulsations observed by the AMPTE CCE magnetic field experiment, *Geophys. Res. Lett., 13,* 905, 1986.

Fedorov, E. N., B. N. Belenkaya, M. B. Gokhberg, S. P. Belokris, L. N. Baransky, and C. A. Green, Magnetospheric plasma density diagnosis from gradient measurements of geomagnetic pulsations, *Planet. Space Sci., 38,* 269, 1990.

Green, A. W., E. W. Worthington, L. N. Baransky, E. N. Fedorov, N. A. Kurneva, V. A. Pilipenko, D. N. Shvetzov, A. A. Bektemirov, and G. V. Philipov, Alfven field line resonances at low latitudes (L=1.5), *J. Geophys. Res., 98,* 15693, 1993.

Gul'yel'mi, A. V., Plasma concentration at great heights according to data on toroidal fluctuations of the magnetosphere, *Geomagn. Aeron., 6,* 98, 1966.

Gul'yel'mi, A. V., The spectrum of Alfven oscillations in the magnetosphere, *Geomagn. Aeron., 10,* 234, 1970.

Hattingh, S. K. F., and P. R. Sutcliffe, Pc3 pulsation eigenperiod determinations at low latitudes, *J. Geophys. Res., 92,* 12433, 1987.

Ho, D., and L. C. Bernard, A fast method to determine the nose frequency and minimum group delay of a whistler when the causative spheric is unknown, *J. Atmos. Terr. Phys., 35,* 881, 1973.

Hughes, W. J., and D. J. Southwood, An illustration of modification of geomagnetic pulsation structure by the ionosphere, *J. Geophys. Res., 81,* 3241, 1976.

Kurchashov, Y. P., Y. S. Nikomarov, V. A. Pilipenko, and A. Best, Field

line resonance effects in local meridional structure of mid-latitude geomagnetic pulsations, *Ann. Geophys., Ser.A,5,* 147, 1987.
Mahajan, K. K., and L. H. Brace, Latitudinal observations of the thermal balance in the nighttime protonosphere, *J. Geophys. Res., 74,* 5099, 1969.
Menk, F. W., B. J. Fraser, C. L. Waters, C. W. S. Ziesolleck, Q. Feng, S. H. Lee, and P. W. McNabb, Ground measurements of low latitude magnetospheric field line resonances, in *Solar Wind Sources of Magnetospheric Ultra-Low-Frequency Waves, Geophys. Monogr. Ser., Vol. 81,* edited by. M. J. Engebretson, K. Takahashi, and M. Scholer, p. 299, AGU, Washington, D.C., 1994.
Menk, F. W., C. L. Waters, and B. J. Fraser, Field line resonances and waveguide modes at low latitudes, 1, Observations, *J. Geophys. Res.,* in press, 1999.
Obayashi, T., Geomagnetic pulsations and the Earth's outer atmosphere, *Rep. Ionos. Space Res. Jpn., 12,* 301, 1958.
Obayashi, T., and J. A. Jacobs, Geomagnetic pulsations and the Earth's outer atmosphere, *Geophys. J. R. Astron. Soc., 1,* 53, 1958.
Olson, J. V., and J. C. Samson, Generalized power spectra and the Stokes vector representations of ultra low frequency micropulsation states, *Can. J. Phys., 58,* 123, 1980.
Orr, D., Magnetospheric hydromagnetic waves: Their eigenperiods, amplitudes and phase variations; A tutorial introduction, *J. Geophys., 55,* 76, 1984.
Orr, D., and J. A. D. Matthew, The variation of geomagnetic micropulsation periods with latitude and the plasmapause, *Planet. Space Sci., 19,* 897, 1971.
Orr, D., and D. C. Webb, Statistical studies of geomagnetic pulsations with periods between 10 and 70 sec and their relationship to the plasmapause region, *Planet. Space Sci., 23,* 1169, 1975.
Park, C. G., Some features of plasma distribution in the plasmasphere deduced from Antarctic whistlers, *J. Geophys. Res., 79,* 169, 1974.
Park, C. G., D. L. Carpenter, and D. B. Wiggin, Electron density in the plasmasphere: Whistler data on solar cycle, annual, and diurnal variations, *J. Geophys. Res., 83,* 3137, 1978.
Pilipenko, V. A., and E. N. Fedorov, Magnetotelluric sounding of the crust and hydromagnetic monitoring of the magnetosphere with the use of ULF waves, in *Solar Wind Sources of Magnetospheric Ultra-Low-Frequency Waves, Geophys. Monogr. Ser.,* Vol. 81, edited by M. J. Engebretson, K. Takahashi, and M. Scholer, p. 283, AGU, Washington D. C., 1994.
Poulter, E. M., W. Allan, G. J. Bailey, and R. J. Moffett, On the diurnal period variation of mid-latitude ULF pulsations, *Planet. Space Sci., 32,* 727, 1984a.
Poulter, E. M., W. Allan, J. G. Keys, and E. Neilsen, Plasmatrough ion mass densities determined from ULF pulsation eigenfrequencies, *Planet. Space Sci., 32,* 1069, 1984b.
Poulter, E. M., W. Allan, and G. J. Bailey, ULF pulsation eigenperiods within the plasmasphere, *Planet. Space Sci., 36,* 185, 1988.
Price, I. A., C. L. Waters, F. W. Menk, G. J. Bailey, and B. J. Fraser, A technique to investigate plasma mass density in the topside ionosphere using ULF waves, *J. Geophys. Res., 104,* 12723, 1999.
Radoski, H. R., The effect of asymmetry on toroidal hydromagnetic waves in a dipole field, *Planet. Space Sci., 20,* 1015, 1972.
Samson, J. C., C. L. Waters, F. W. Menk, and B. J. Fraser, Fine structure in the spectra of low latitude field line resonances, *Geophys. Res. Lett., 22,* 2111, 1995.
Saxton, J. M., and A. J. Smith, Quiet time plasmaspheric electric fields and plasmasphere-ionosphere coupling fluxes at L=2.5, *Planet. Space Sci., 37,* 283, 1989.
Singer, H. J., D. J. Southwood, R. J. Walker, and M. G. Kivelson, Alfven wave resonances in a realistic magnetospheric magnetic field geometry, *J. Geophys. Res., 86,* 4589, 1981.
Smith, R. L., and J. J. Angerami, Magnetospheric properties deduced from Ogo 1 observations of ducted and nonducted whistlers, *J. Geophys. Res., 73,* 1, 1968.
Smith, A. J., and M. A. Clilverd, Magnetic storm effects on the mid-latitude plasmasphere, *Planet. Space Sci., 39,* 1069, 1991.
Smith, A. J., K. H. Yearby, K. Bullough, J. M. Saxton, H. J. Strangeways, and N. R. Thomson, Whistler mode signals from VLF transmitters located at Faraday, Antarctica, *Mem. Natl. Inst. Polar Res., 48,* 183, 1987.
Takahashi, K., and B. J. Anderson, Distribution of ULF energy (f<80 mHz) in the inner magnetosphere: A statistical analysis of AMPTE CCE magnetic field data, *J. Geophys. Res., 97,* 10751, 1992.
Takahashi, K., and R. L. McPherron, Harmonic structure of Pc3-4 pulsations, *J. Geophys. Res., 87,* 1504, 1982.
Tamao, T., Transmission and coupling resonance of hydromagnetic disturbances in the non-uniform Earth's magnetosphere, *Sci. Rep. Tohoku Univ., Ser. 5, 17,* 43, 1966.
Taylor, J. P. H., and A. D. M. Walker, Accurate approximate formulae for toroidal standing hydromagnetic oscillations in a dipolar geomagnetic field, *Planet. Space Sci., 32,* 1119, 1984.
Thomson, N. R., Whistler mode signals: Spectrographic group delays, *J. Geophys. Res., 86,* 4795, 1981.
Troitskaya, V. A., and A. V. Gul'yel'mi, Hydromagnetic diagnostics of plasma in the magnetosphere, *Ann. Geophys., 26,* 893, 1970.
Tsyganenko, N.A., Global quantative models of the geomagnetic field in the cislunar magnetosphere for different disturbance levels, *Planet. Space Sci., 35,* 1347, 1987.
Vellante, M., U. Villante, R. Core, A. Best, D. Lenners, and V. A. Pilipenko, Simultaneous geomagnetic pulsation observations at two latitudes: Resonant mode characteristics, *Ann. Geophys., 11,* 734, 1993.
Vellante, M., U. Villante, M. De Lauretis, and G. Barchi, Solar cycle variation of the dominant frequencies of Pc 3 geomagnetic pulsations at L=1.6, *Geophys. Res. Lett., 23,* 1505, 1996.
Verõ., J. H. Lühr, M.Vellante, I. Best, J. Střeštik, J. C. Miletits, L. Holló, J. Szendrõi, and B. Ziegler, Upstream waves and field line resonances: Simultaneous presence and alternation in Pc3 pulsation events, *Ann. Geophys., 16,* 34, 1998.
Walker, A. D. M., Formation of whistler ducts, *Planet. Space Sci., 26,* 375, 1978.
Walker, A. D. M., J. M. Ruohoniemi, K. B. Baker, R. A. Greenwald, and J. C. Samson, Spatial and temporal behavior of ULF pulsations observed by the Goose Bay HF radar, *J. Geophys. Res., 97,* 12187, 1992.
Walker, R. J., and C. T. Russell, Solar-wind interactions with magnetized planets, in *Introduction to Space Physics,* edited by M. G. Kivelson and C. T. Russell, p. 164, Cambridge Univ. Press, New York, 1995.
Warner, M. R., and D. Orr, Time of flight calculations for high latitude geomagnetic pulsations, *Planet. Space Sci., 27,* 679, 1979.
Waters, C. L., F. W. Menk, and B. Fraser, The resonance structure of low latitude Pc3 geomagnetic pulsations, *Geophys. Res. Lett., 18,* 2293, 1991.
Waters, C. L., F. W. Menk, and B. J. Fraser, Low latitude geomagnetic field line resonance: Experiment and modeling, *J. Geophys. Res., 99,* 17547, 1994.
Waters, C. L., J. C. Samson, and E. F. Donovan, The temporal variation of the frequency of high latitude field line resonances, *J. Geophys. Res., 100,* 7987, 1995.
Waters, C. L., B. G. Harrold, F. W. Menk, J. C. Samson, and B. J. Fraser, Field line resonances and waveguide modes at low latitudes, 2, A model, *J. Geophys. Res.,* in press, 1999.
Webb, D. C., L. J. Lanzerotti, and C. G. Park, A comparison of ULF and VLF measurements of magnetospheric cold plasma densities, *J. Geophys. Res., 82,* 5063, 1977.
Yeoman, T. K., D. K. Milling, and D. Orr, Pi2 polarization patterns on the U. K. Sub-Auroral Magnetometer Network (SAMNET), *Planet. Space Sci., 38,* 589, 1990.

M. A. Cliverd and A. J. Smith, British Antarctic Survey, Madingley Road, Cambridge CB 3 OET, England, U. K.
B. J. Fraser, F. W. Menk, and C. L. Waters, Department of Physics, University of Newcastle, University Drive, Callaghan, Newcastle, N. S. W. 2308, Australia. (email: physpuls3@cc.newcastle.edu.au)
D. K. Milling and D. Orr, Department of Physics, University of York, Heslington, York YO1 5DD, England, U. K.

(Received November 2, 1998; revised April 25, 1999; accepted April 30, 1999.)